NEURAL REGENERATION RESEARCH
December 2017, Volume 12, Issue 12
www.nrronline.org

RESEARCH ARTICLE

Diffusion tensor imaging of spinal microstructure in healthy adults: improved resolution with the readout segmentation of long variable echo-trains

Bu-tian Zhang, Meng Li, Li-li Yu, Yi-meng Dai, Shao-nan Yu, Jin-lan Jiang*
China-Japan Union Hospital of Jilin University, Changchun, Jilin Province, China

How to cite this article: *Zhang BT, Li M, Yu LL, Dai YM, Yu SN, Jiang JL (2017) Diffusion tensor imaging of spinal microstructure in healthy adults: improved resolution with the readout segmentation of long variable echo-trains. Neural Regen Res 12(12):2067-2070.*

Graphical Abstract

The readout segmentation of long variable echo-trains (RESOLVE) sequence improves the resolution of diffusion tensor imaging (DTI) image in clinical application

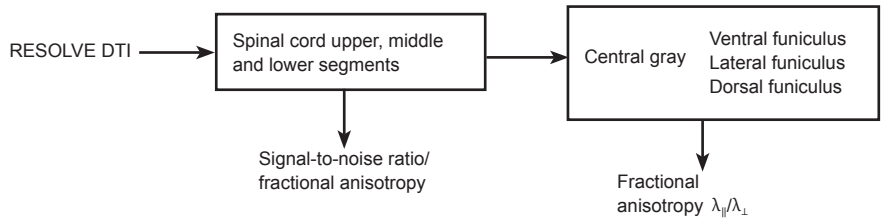

Correspondence to:
Jin-lan Jiang, M.D., zbt0417@outlook.com; jiangjl2003@hotmail.com.

orcid:
0000-0003-0891-3464 (Jin-lan Jiang)

doi: *10.4103/1673-5374.221166*

Accepted: *2017-09-18*

Abstract

Diffusion tensor imaging plays an important role in the accurate diagnosis and prognosis of spinal cord diseases. However, because of technical limitations, the imaging sequences used in this technique cannot reveal the fine structure of the spinal cord with precision. We used the readout segmentation of long variable echo-trains (RESOLVE) sequence in this cross-sectional study of 45 healthy volunteers aged 20 to 63 years. We found that the RESOLVE sequence significantly increased the resolution of the diffusion images and improved the median signal-to-noise ratio of the middle ($C_{4–6}$) and lower (C_7–T_1) cervical segments to the level of the upper cervical segment. In addition, the values of fractional anisotropy and radial diffusivity were significantly higher in white matter than in gray matter. Our study verified that the RESOLVE sequence could improve resolution of diffusion tensor imaging in clinical applications and provide accurate baseline data for the diagnosis and treatment of cervical spinal cord diseases.

Key Words: *nerve regeneration; diffusion tensor imaging; cervical spinal cord; microstructure; gray matter; white matter; readout segmentation of long variable echo-train sequence; signal-to-noise ratio; fractional anisotropy; neural regeneration*

Introduction

Diffusion tensor imaging (DTI) is an advanced noninvasive magnetic resonance imaging (MRI) method that can qualitatively and quantitatively analyze the diffusion of water within a voxel in three-dimensional space (Sąsiadek et al., 2012). Because of the sheath's structure, water molecules tend to move along the longitudinal axis of axons in neural tissues (Beaulieu, 2002). This feature strongly favors the utility of DTI for the assessment of spinal cord diseases. A previous study has reported that DTI can detect cord damage, which is easily misdiagnosed on T2-weighted images (Banaszek et al., 2014). Most research has generally focused on clinical applications (Demir et al., 2003; Petersen et al., 2012; Ellingson et al., 2014). Only a few studies have focused on the detailed structure of the spinal cord, and most did not precisely characterize the anatomical microstructure because of the confined spatial resolution or relatively low signal-to-noise ratio (SNR) (Rossi et al., 2008). The low SNR also affected the accuracy of DTI parameters (Jones and Basser, 2004). DTI is useful in clinical diagnosis and outcome assessment of patients with cervical cord diseases, and it is necessary to establish the baseline microstructure of the cervical spinal cord with a high spatial resolution DTI sequence.

The readout segmentation of long variable echo-trains (RESOLVE) sequence is a novel scanning magnetic resonance (MR) technique, based on a readout segmented echo planar imaging (EPI) strategy. Our study applied RESOLVE sequences with DTI techniques to improve image quality at the technical level and to clearly distinguish gray matter and white matter funiculi of the spinal cord in a large number of healthy individuals. We collected foundation data for the further study of cervical spinal cord diseases.

Participants and Methods

Participants

We studied 45 healthy, asymptomatic subjects from the

physical examination center of our hospital: 19 men and 26 women with ages ranging from 20 to 63 years (average 39.15 years). Participants underwent a neurological evaluation and MRI. In this cross-sectional study, patients with neurological disorders, congenital spinal canal narrowing, central spinal canal widening, previous spinal surgery, and those with any incidental findings on plain MR images suggestive of a neurological disorder were excluded from this study. The study protocols were approved by the Ethics Committee of China-Japan Union Hospital of Jilin University of China. The research followed the international and national guidelines in accordance with the procedures of the *Helsinki Declaration* of 1975 as revised in 2000. All voluntary participants were fully informed about the experimental process, and provided signed consent.

Image acquisition

MR examinations were performed with a 3.0 Tesla (T) clinical MR scanner (MAGNETOM Skyra; Siemens Medical Systems, Berlin, Germany), using a 32-channel coil dedicated to neck and head imaging (Siemens Medical Systems). The MR protocol consisted of a sagittal T1-weighted image (T1WI; repetition time/echo time = 600/20 ms), sagittal T2-weighted image (T2WI; repetition time/echo time = 2,800/120 ms), sagittal proton density-weighted image (repetition time/echo time = 2,600/15 ms), and axial proton density-weighted image (repetition time/echo time = 2,700/20 ms), followed by an axial DTI sequence.

The DTI sequence was acquired using the RESOLVE sequence over the entire cervical spine (C_1–T_1). Diffusion weighted images were obtained using the following scanning parameters: (1) axial slices were acquired to distinguish white matter and gray matter, which was perpendicular to the spinal cord with diffusion gradients in 20 equidistant directions with a b = 1,000 s/mm^2; (2) phase encoding direction, anterior-posterior; (3) repetition time/echo time = 2,800/89 ms; (4) slice thickness = 3 mm; (5) number of slices = 15; (6) interslice gap = 0 mm; (7) number of excitations = 2; (8) matrix size = 256 × 256; field of view = 220 mm × 220 mm; (9) generalized autocalibrating partially parallel acquisitions acceleration factor = 2; and (10) readout segments = 5. The total acquisition time was controlled at an appropriate level of 6 minutes and 39 seconds.

Regions of interest (ROIs)

DTI images were processed using Neuro 3D engine on a Siemens workstation, and three slices per cervical level were selected for analysis. Five fields of view for each slice were covered on the ventral, lateral, and dorsal funiculi as well as the central gray substance on axial T2WI images. Then the ROI information was coregistered to all maps of DTI parameters with MRIcron software (McCausland Center for Brain Imaging of University of South Carolina, Columbia, SC, USA) (**Figure 1**). The small ROIs were designed with at least two voxels inside the cord edge to avoid the partial volume effect of cerebrospinal fluid. The measurement results of the right and left lateral funiculi were averaged.

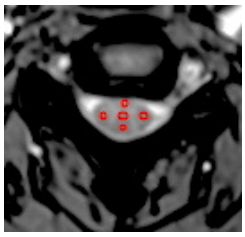

Figure 1 Axial slice of the cervical spinal cord of a 28-year-old man.
Five regions of interest were covered on T2-weighted image and coregistered with all diffusion tensor imaging parameters images. Two voxels at least were apart from the edge of spinal cord to avoid contamination of regions of interest by cerebrospinal fluid. Red circle: Regions of interest.

Three regions were defined in the cervical cord: upper segment (upper border of C_1–lower border of C_3), middle segment (upper border of C_4–lower border of C_6), and lower segment (upper border of C_7–lower border of T_1) (**Figure 2**). The SNR of all the cervical spinal cord regions was calculated from b = 1,000 s/mm^2 images. Signal ROIs were selected at a consistent location inside the body, while noise ROIs were selected in air, and were obtained at least 10 voxels away from the borders of the image.

Data processing

SNR and DTI parameters of all levels were estimated and analyzed on a Siemens workstation. The median SNR of each region was calculated using the following equations:

$$SNR=SI(spinal)/SD(air)$$

where SI is signal intensity and SD is standard deviation.

Fractional anisotropy (FA), apparent diffusion coefficient and three eigenvalues (λ_1, λ_2, λ_3) were derived from each ROI. Axial diffusivity ($\lambda_{\parallel}$) and radial diffusivity ($\lambda_{\perp}$) were calculated using the following equations:

$$\lambda_{\parallel}=\lambda_1$$
$$\lambda_{\perp}=\frac{1}{2}(\lambda_2+\lambda_3)$$

Axial diffusivity is correlated with axon diameter, and radial diffusivity is positively correlated with axon spacing. Both of them reflect distinct histological parameters and characterize tissue integrity beyond the general measure of anisotropic water diffusion with additional information.

Statistical analysis

Statistical analysis was performed using IBM SPSS Statistics for Windows, Version 22.0 (IBM Corp., Armonk, NY, USA). To compare the SNR data of each region, Mann-Whitney U test was used. The difference was determined between left and right lateral funiculi by Student's t-test. One-way analysis of variance was used to compare DTI measures of spinal fibers, and Tukey's *post hoc* test was performed to compare subgroups of each funiculus. Data were recorded as the mean ± SD. A value of $P < 0.05$ was considered statistically significant.

Results

We enrolled 50 participants in the study, 5 participants were excluded because routine neurological exam was positive. The residual participants showed significant cord disease on T2WI and proton density–weighted image. All of the axial DTI parameter maps were compared with the corresponding axial T2WI in a representative subject.

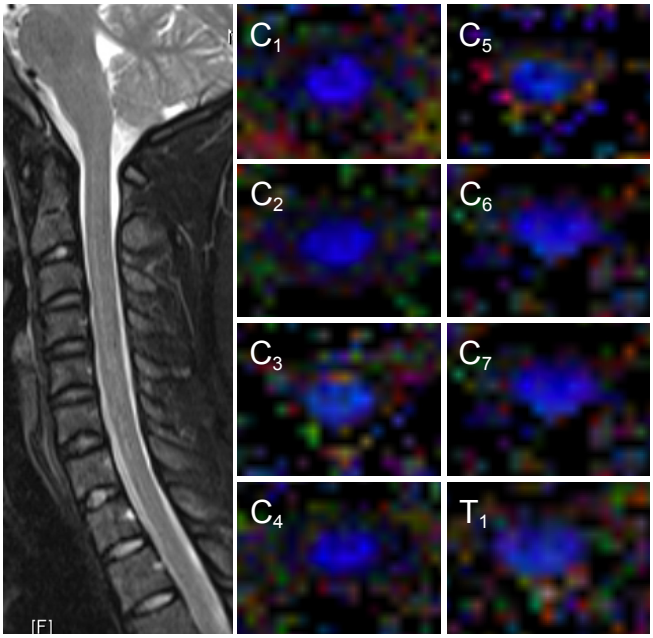

Figure 2 Axial fractional anisotropy maps and T2-weighted images at individual levels of the cervical spinal cord of a 28-year-old man. Images were obtained with a Siemens SKYRA 3.0T clinical magnetic resonance scanner. CoFA maps show higher anisotropy in the white matter funiculi than in the central gray matter. C_{1-7}: Cervical vertebrae 1−7; T_1: thoracic vertebra 1. FA: Fractional anisotropy.

Table 1 Signal-to-noise ratio and fractional anisotropy values of each cervical spinal cord segment

Segment	SNR	FA
Upper	7.6±1.2	0.78±0.02**
Middle	7.3±0.9	0.67±0.05**
Lower	7.4±1.1	0.68±0.02

Upper segment: Upper border of C_1–lower border of C_3, middle segment: upper border of C_4–lower border of C_6, lower segment: upper border of C_7–lower border of T_1. Data are recorded as the mean ± SD. Signal-to-noise ratio (SNR) is analyzed by the Mann-Whitney *U* test ($P = 0.13$), and fractional anisotropy (FA) is analyzed by one-way analysis of variance followed by Tukey's *post hoc* test. The difference between the left and right lateral funiculi was determined by Student's *t*-test. **$P < 0.01$, *vs.* lower segment.

SNR

The median SNR of the diffusion images was 7.3 across all levels. The median SNR of the upper, middle, and lower cervical cord segments are shown in **Table 1**. The SNR had no significant difference in different segments of the cervical spinal cord (Mann-Whitney *U* test; $P = 0.13$).

White matter and gray matter

The mean FA, $\lambda_{\parallel}$ and $\lambda_{\perp}$ of all white matter tracts and gray matter are shown in **Tables 1** and **2**. There was no significant difference between left and right lateral funiculi; therefore, we combined both lateral funiculi as one group with average data. The whole-cord FA of the upper group was higher than in other groups ($P = 0.00 < 0.01$) (**Table 1**). The $\lambda_{\parallel}$ of the ventral funiculi in all groups was higher than other regional funiculi ($P = 0.003 < 0.01$) (**Table 2**). The FA and $\lambda_{\perp}$ of the gray matter were significantly lower than in the white matter ($P = 0.004 < 0.01$). **Table 2** shows each regional difference between DTI parameters of gray matter and individual white matter funiculi.

Discussion

Diffusivities of gray and white matter in the normal human spinal cord have been measured and evaluated (Onu et al., 2010). However, important limitations of DTI for the cervical spinal cord have emerged. Because of the poor spatial resolution and little data, DTI parameters of the individual white matter funiculi were found to be inaccurate (Ellingson et al., 2007). In other reports, because of an underestimation of diffusion anisotropy, the results of DTI parameters were affected by the SNR (Dietrich et al., 2001; Jones and Basser, 2004). In our study, RESOLVE sequencing was used with the preliminary DTI technique and then verified to improve the spatial resolution and SNR in the cervical spinal cord. Compared with other DTI sequences, the RESOLVE sequence is based on the multishot EPI, including a sampling stand readout segmental EPI and a 2D navigate echo, which could minimize phase-encode distortion artifacts and $T2^*$ blurring through fast k-space filling, while SNR efficiency increases substantially (Frost et al., 2014). This sequence could also be combined with the generalized autocalibrating partially parallel acquisitions technique, which could allow direct reduction of the acquisition time (Yamada et al., 2016). Because of these advantages, this sequence is clearly beneficial and demonstrates FA differences; further, sequences provide better results in a short time period (Banaszek et al., 2014; Middleton et al., 2014), even though the images are not as visually impressive. The SNR of all segmental groups of the cervical spinal cord was improved in our study, especially in the lower group, which was easily affected by swallowing or body morphology. Therefore, the accuracy of all DTI parameters significantly improved.

In our study, the effect of SNR was minimized, and the trend in SNR values across the cervical spinal cord was uniform. However, the whole-cord FA value of the upper cervical group was still higher than in the middle group and the lower group. This result may involve the fiber density, which correlated with extracellular spaces (Takahashi et al., 2002; Ong et al., 2008). Because of cervical enlargement, the fiber density of the upper group may be higher than in the middle and lower groups. The mean white matter FA value in the cervical cord was similar to that in some previous reports, and the larger sample size of our study could explain minor variations in DTI parameters. Similar to the study by Vedantam et al. (2013), our results revealed that significant differences between the FA in each area of individual white funiculi and the FA value of ventral funiculi were lowest compared with lateral and dorsal funiculi through all the white matter bundles. We also found that axial diffusion was highest in the ventral funiculi. Previous studies suggest that radial diffusivity strongly associates with the diameter of axons and to the fiber packing density. For example, the vestibulospinal tract with the largest axons also had the highest radial diffusivity values (Schwartz et al., 2005). Thus, axon diameter of the ventral funiculi increases and axons are less

Table 2 Fractional anisotropy, $\lambda_{\parallel}$ and $\lambda_{\perp}$ values of all regions of interest of each cervical spinal cord segment

Segment	DTI metrics	Ventral funiculus	Lateral funiculus	Dorsal funiculus	Central gray matter
Upper	FA(a)	0.73±0.09††	0.80±0.03††	0.77±0.01††	0.53±0.03
	$\lambda_{\parallel}$(b)	1.66±0.20	1.77±0.09	1.56±0.27	1.59±0.02
	$\lambda_{\perp}$(c)	0.31±0.05††	0.37±0.02$^{\#\#\dagger\dagger}$	0.40±0.08$^{\#\#\dagger\dagger}$	0.66±0.04
Middle	FA(a)	0.70±0.01††	0.75±0.08††	0.73±0.02††	0.51±0.05
	$\lambda_{\parallel}$(b)	1.78±0.13	1.60±0.20	1.64±0.08	1.74±0.40
	$\lambda_{\perp}$(c)	0.36±0.01††	0.38±0.03$^{\#\#\dagger\dagger}$	0.42±0.06$^{\#\#\dagger\dagger}$	0.70±0.09
Lower	FA(a)	0.68±0.02††	0.76±0.02††	0.69±0.03††	0.54±0.03
	$\lambda_{\parallel}$(b)	1.65±0.28	1.59±0.07	1.73±0.17	1.66±0.25
	$\lambda_{\perp}$(c)	0.34±0.02††	0.39±0.04$^{\#\#\dagger\dagger}$	0.44±0.05$^{\#\#\dagger\dagger}$	0.68±0.07

Upper segment: Upper border of C_1–lower border of C_3; middle segment: upper border of C_4–lower border of C_6; lower segment: upper border of C_7–lower border of T_1. Data are recorded as the mean ± SD and analyzed by one-way analysis of variance followed by Tukey's *post hoc* test. ##P < 0.01, *vs.* ventral funiculus; ††P < 0.01, *vs.* central gray matter. FA: Fractional anisotropy.

densely packed relative to the lateral and dorsal funiculi. The general pattern of gray matter is similar to that reported by Onu et al. (2010), and the FA of gray matter is lower than that of white matter through the whole cervical spinal cord.

In conclusion, the RESOLVE sequence improves spatial resolution of DTI imaging in clinical applications and provides DTI baseline data for the gray matter and different white matter funiculi throughout the cervical spinal cord.

Author contributions: *BTZ participated in study design and paper writing. ML, LLY, YMD, and SNY were in charge of data collection. JLJ gave research guidance. All authors approved the final version of the paper.*
Conflicts of interest: *None declared.*
Research ethics: *The study protocol was approved by Ethics Committee of China-Japan Hospital of Jilin University. The study followed international and national regulations in accordance with the Declaration of Helsinki. Written informed consent was provided by each participant after they indicated that they had fully understood the treatment plan.*
Declaration of participant consent: *The authors certify that they have obtained all appropriate participant consent forms. In the form, participants have given their consent for their images and other clinical information to be reported in the journal. Participants understand that their names and initials will not be published and while due efforts will be made to conceal their identity, anonymity cannot be guaranteed.*
Data sharing statement: *Datasets analyzed during the current study are available from the corresponding author on reasonable request.*
Plagiarism check: *Checked twice by iThenticate.*
Peer review: *Externally peer reviewed.*

References

Banaszek A, Bladowska J, Szewczyk P, Podgorski P, Sasiadek M (2014) Usefulness of diffusion tensor MR imaging in the assessment of intramedullary changes of the cervical spinal cord in different stages of degenerative spine disease. Eur Spine J 23:1523-1530.

Beaulieu C (2002) The basis of anisotropic water diffusion in the nervous system - a technical review. NMR Biomed 15:435-455.

Demir A, Ries M, Moonen CT, Vital JM, Dehais J, Arne P, Caillé JM, Dousset V (2003) Diffusion-weighted MR imaging with apparent diffusion coefficient and apparent diffusion tensor maps in cervical spondylotic myelopathy. Radiology 229:37-43.

Dietrich O, Heiland S, Sartor K (2001) Noise correction for the exact determination of apparent diffusion coefficients at low SNR. Magn Reson Med 45:448-453.

Ellingson BM, Ulmer JL, Schmit BD (2007) Gray and white matter delineation in the human spinal cord using diffusion tensor imaging and fuzzy logic. Acad Radiol 14:847-858.

Ellingson BM, Salamon N, Grinstead JW, Holly LT (2014) Diffusion tensor imaging predicts functional impairment in mild-to-moderate cervical spondylotic myelopathy. Spine J 14:2589-2597.

Frost R, Jezzard P, Douaud G, Clare S, Porter DA, Miller KL (2014) Scan time reduction for readout-segmented EPI using simultaneous multislice acceleration: Diffusion-weighted imaging at 3 and 7 Tesla. Magn Reson Med doi: 10.1002/mrm.25391.

Jones DK, Basser PJ (2004) "Squashing peanuts and smashing pumpkins": how noise distorts diffusion-weighted MR data. Magn Reson Med 52:979-993.

Middleton DM, Mohamed FB, Barakat N, Hunter LN, Shellikeri S, Finsterbusch J, Faro SH, Shah P, Samdani AF, Mulcahey MJ (2014) An investigation of motion correction algorithms for pediatric spinal cord DTI in healthy subjects and patients with spinal cord injury. Magn Reson Imaging 32:433-439.

Ong HH, Wright AC, Wehrli SL, Souza A, Schwartz ED, Hwang SN, Wehrli FW (2008) Indirect measurement of regional axon diameter in excised mouse spinal cord with q-space imaging: simulation and experimental studies. Neuroimage 40:1619-1632.

Onu M, Gervai P, Cohen-Adad J, Lawrence J, Kornelsen J, Tomanek B, Sboto-Frankenstein UN (2010) Human cervical spinal cord funiculi: investigation with magnetic resonance diffusion tensor imaging. J Magn Reson Imaging 31:829-837.

Petersen JA, Wilm BJ, von Meyenburg J, Schubert M, Seifert B, Najafi Y, Dietz V, Kollias S (2012) Chronic cervical spinal cord injury: DTI correlates with clinical and electrophysiological measures. J Neurotrauma 29:1556-1566.

Rossi C, Boss A, Steidle G, Martirosian P, Klose U, Capuani S, Maraviglia B, Claussen CD, Schick F (2008) Water diffusion anisotropy in white and gray matter of the human spinal cord. J Magn Reson Imaging 27:476-482.

Sąsiadek MJ, Szewczyk P, Bladowska J (2012) Application of diffusion tensor imaging (DTI) in pathological changes of the spinal cord. Med Sci Monit 18:RA73-79.

Schwartz ED, Cooper ET, Fan Y, Jawad AF, Chin CL, Nissanov J, Hackney DB (2005) MRI diffusion coefficients in spinal cord correlate with axon morphometry. Neuroreport 16:73-76.

Takahashi M, Hackney DB, Zhang G, Wehrli SL, Wright AC, O'Brien WT, Uematsu H, Wehrli FW, Selzer ME (2002) Magnetic resonance microimaging of intraaxonal water diffusion in live excised lamprey spinal cord. Proc Natl Acad Sci U S A 99:16192-16196.

Vedantam A, Jirjis MB, Schmit BD, Wang MC, Ulmer JL, Kurpad SN (2013) Characterization and limitations of diffusion tensor imaging metrics in the cervical spinal cord in neurologically intact subjects. J Magn Reson Imaging 38:861-867.

Yamada H, Yamamoto A, Okada T, Kanagaki M, Fushimi Y, Porter DA, Tanji M, Hojo M, Miyamoto S, Togashi K (2016) Diffusion tensor imaging of the optic chiasm in patients with intra- or parasellar tumor using readout-segmented echo-planar. Magn Reson Imaging 34:654-661.

Copyedited by Yu J, Li CH, Qiu Y, Song LP, Zhao M